Nanomechanics driven by Andreev tunneling

A. V. Parafilo,[1,*] L. Y. Gorelik,[2] M. V. Fistul,[1,3,4] H. C. Park,[1,†] and R. I. Shekhter[5]

[1]*Center for Theoretical Physics of Complex Systems, Institute for Basic Science, Expo-ro, 55, Yuseong-gu, Daejeon 34126, Republic of Korea*
[2]*Department of Physics, Chalmers University of Technology, SE-412 96 Göteborg, Sweden*
[3]*Theoretische Physik III, Ruhr-University Bochum, Bochum 44801 Germany*
[4]*National University of Science and Technology "MISIS", Russian Quantum Center, Moscow 119049, Russia*
[5]*Department of Physics, University of Gothenburg, SE-412 96 Göteborg, Sweden*

(Received 9 September 2020; revised 10 November 2020; accepted 16 November 2020; published 1 December 2020)

We predict and analyze mechanical instability and corresponding self-sustained mechanical oscillations occurring in a nanoelectromechanical system composed of a metallic carbon nanotube (CNT) suspended between two superconducting leads and coupled to a scanning tunneling microscope (STM) tip. We show that such phenomena are realized in the presence of both the coherent Andreev tunneling between the CNT and superconducting leads, and an incoherent single electron tunneling between the voltage biased STM tip and CNT. Treating the CNT as a single-level quantum dot, we demonstrate that the mechanical instability is controlled by the Josephson phase difference, relative position of the electron energy level, and the direction of the charge flow. It is found numerically that the emergence of the self-sustained oscillations leads to a substantial suppression of DC electric current.

DOI: 10.1103/PhysRevB.102.235402

I. INTRODUCTION

Modern nanomechanical resonators [1] characterized by low damping and fine tuning of the resonant frequency are widely used nowadays as supersensitive quantum detectors [2–6] and as the mechanical component for various nanoelectromechanical systems (NEMS) [7,8]. The latter represent a promising platform for studying the fundamental phenomena generated by the quantum-mechanical interplay between nanomechanical resonator and electronic subsystem [9,10].

Large amount of fascinating physical phenomena have been predicted and observed in various NEMS, e.g., energy level quantization of a nanomechanical oscillator [11], a strong resonant coupling of nanomechanical oscillator to superconducting qubits [12,13], mechanical cooling [14–16], a single-atom lasing effect [12,17], mechanical transportation of Cooper pairs [18], and the generation of self-driven mechanical oscillations by a DC charge flow [19–24], just to name a few.

A significant part of these effects is based on the resonant excitation of low damped mechanical modes by *coherent* quantum dynamics occurring in the electronic subsystem. A straightforward method to establish coherent quantum dynamics in mesoscopic devices, e.g., the quantum beats, the microwave induced Rabi oscillations, etc., is to use the macroscopic phase coherence of superconducting (SC) elements incorporated into NEMS [25,26]; see also, for example, the review [27]. In particular, in superconducting hybrid junctions [28–35] the coherent electronic transport is determined by the presence of Andreev bound states [36,37]. The applied DC or AC currents induce the transitions between Andreev bound states, and the coherent high-frequency oscillations in an electronic subsystem occur [15,38–40]. These coherent charge oscillations can excite the mechanical modes in the resonant limit only, when the frequency of mechanical mode matches Andreev energy level difference [15].

On the other hand, an *incoherent* quantum dynamics occurring in the electronic subsystem can induce the mechanical instability and subsequent formation of the self-driven mechanical oscillations in hybrid junctions. Incoherent quantum fluctuations of electric charge can be easily mediated by tunneling of a single electron. The self-driven oscillations generated by a DC electronic flow have been predicted in Refs. [19,20], later observed in a carbon nanotube (CNT) based transistor [21] and studied in detail [22,23]; see, e.g., Ref. [24] for a recent experiment. A nontrivial interplay between coherent and incoherent electric charge variation and its influence on the performance of NEMS can be achieved in a *nanomechanical Andreev device*, where normal and SC metals are bridged by a mechanically active mediator.

In this paper, we present a particular NEMS setup where the mechanical oscillations are strongly affected by a weak coupling to the electronic part of a system. We demonstrate that in the adiabatic limit as the frequency of mechanical oscillations is much smaller than the typical frequencies of electron dynamics, simultaneous presence of coherent Andreev tunneling and incoherent single electron tunneling can induce mechanical instability of the resonator and result in the appearance of the self-sustained mechanical oscillations.

The paper is organized as follows: Section II is devoted to formulation of the model describing the nanomechanical Andreev device. The effective Newton's equation of the

*aparafil@ibs.re.kr
†hc2725@gmail.com

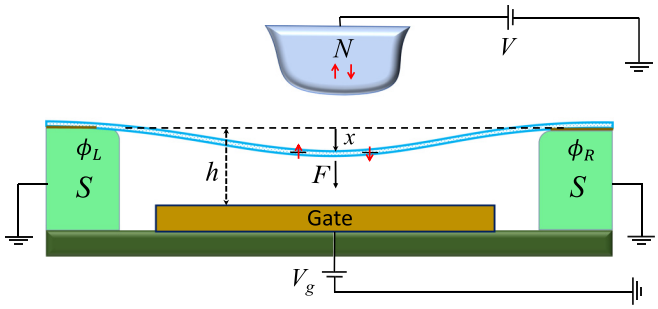

FIG. 1. Scheme of the superconducting (SC) nanoelectromechanical device. A single-wall carbon nanotube (CNT) is suspended between two SC leads which are characterized by the phases of SC order parameter, $\phi_{L,R}$. A normal metal electrode (STM tip) placed near the CNT-QD allows us to inject electrons in CNT. The nanoelectromechanical force F between the CNT and gate electrode, which is located on the distance h from the CNT, is controlled by a gate voltage V_g.

mechanical resonator is analyzed as well as the criterion of the mechanical instability is discussed in Sec. III. The DC electric current in the considered device is numerically studied in Sec. IV. The summary and discussions are given in Sec. V.

II. MODEL

We consider a metallic single-wall carbon nanotube suspended between two grounded SC electrodes [26] and coupled to a scanning tunneling microscope (STM) tip via electron tunneling. The two SC electrodes are characterized by the same modulus Δ and different phases $\phi_{L,R}$ of SC order parameter, and corresponding Josephson phase difference $\phi = \phi_R - \phi_L$. We study the case where the CNT mean-level spacing is greater than temperature k_BT and the bias voltage eV applied between STM tip and CNT. It allows us to treat the CNT as a movable single-level quantum dot (QD). The capacitive coupling between the CNT and a gate is controlled by a gate voltage V_g. We also assume the dynamics of the CNT bending is reduced to the dynamics of the fundamental flexural mode. The scheme of the described model is presented in Fig. 1.

The Hamiltonian of the model reads as follows

$$H = H_N + H_S + H_{\rm CNT} + H_{\rm tun}. \tag{1}$$

The first two terms in Eq. (1) are the Hamiltonians of an STM tip (normal lead) and two SC leads, accordingly:

$$H_N = \sum_{k\sigma} (\varepsilon_k - eV) c^\dagger_{k\sigma} c_{k\sigma}, \tag{2}$$

$$H_S = \sum_{kj\sigma} \{\xi_{kj} a^\dagger_{kj\sigma} a_{kj\sigma} - \Delta e^{i\phi_j} (a^\dagger_{kj\uparrow} a^\dagger_{-kj\downarrow} + \text{H.c.})\}. \tag{3}$$

Here, $c_{k\sigma}$ ($c^\dagger_{k\sigma}$) and $a_{kj\sigma}$ ($a^\dagger_{kj\sigma}$) are annihilation (creation) operators of electrons in the normal and jth SC leads ($j = L, R$) with energies ε_k and ξ_{kj}, correspondingly. The index $\sigma = \uparrow, \downarrow$ indicates the spin of electrons in the leads.

The Hamiltonian of the single-level vibrating CNT-QD reads as follows

$$H_{\rm CNT} = \sum_\sigma \varepsilon_0 d^\dagger_\sigma d_\sigma + \frac{\hbar\omega_0}{2}(\hat{p}^2 + \hat{x}^2) - F\hat{x}\sum_\sigma n_\sigma. \tag{4}$$

The quantum dynamics of the electronic degree of freedom is described by the first term in Eq. (4), where ε_0 is the QD electron energy level, and d_σ, $d^\dagger_\sigma$ are annihilation and creation operators of the electrons in the QD, $n_\sigma = d^\dagger_\sigma d_\sigma$. We omit the interdot electron interaction $U n_\uparrow n_\downarrow$ in the case when $U < eV$, since it will give only qualitative correction to the phenomenon under consideration. More precisely, it will result in renormalization of the QD energy level, $\varepsilon_0 \to \varepsilon_0 + U/2$.

The second term in Eq. (4) characterizes the CNT vibrations with the frequency ω_0, and the dimensionless operators $\hat{x} = \hat{X}/x_0$, $\hat{p} = x_0\hat{P}/\hbar$ are canonically conjugated displacement and momentum of the CNT-QD. Here, $x_0 = \sqrt{\hbar/m\omega_0}$ is the amplitude of the zero-point oscillations of the CNT, and m is the mass of the CNT. Electromechanical interaction determined by the third term in Eq. (4) is achieved through the electrostatic interaction of the charged CNT-QD with the gate electrode. The interaction strength is $F \propto (ex_0/h)V_g\beta$ [20,41], where h is the distance between the CNT and gate electrode, and $\beta \sim 0.1$ is a geometrical factor associated with the capacitances in the system.

The last term in Eq. (1),

$$H_{\rm tun} = \sum_{k\sigma} e^{-\hat{x}/\lambda}\left(t^n_k c^\dagger_{k\sigma} d_\sigma + (t^n_k)^* d^\dagger_\sigma c_{k\sigma}\right) + \sum_{kj\sigma}\left(t^s_k a^\dagger_{kj\sigma} d_\sigma + \left(t^s_k\right)^* d^\dagger_\sigma a_{kj\sigma}\right), \tag{5}$$

describes the tunneling processes between the CNT and (i) the STM tip with deflection dependent hopping amplitude, i.e., $t^n_k \exp(-\hat{x}/\lambda)$, where $\lambda = l/x_0$ and l is the tunneling length of the barrier; (ii) SC leads with the hopping amplitude t^s_k.

III. MECHANICAL INSTABILITY

In order to rigorously demonstrate the phenomenon of mechanical instability in the SC hybrid junction, we analyze the dynamics of the CNT's flexural mode by using the reduced density matrix technique. By treating the tunneling Hamiltonian (5) as a perturbation and tracing out the electronic degrees of freedom in the normal and SC leads, one can get a quantum master equation for the reduced density matrix operator (in $\hbar = 1$ units):

$$\dot{\rho} = -i[H_{\rm CNT}, \rho] + i\Gamma_S(\phi)[d^\dagger_\uparrow d^\dagger_\downarrow + d_\downarrow d_\uparrow, \rho] - \sum_\sigma \mathcal{L}[\rho]. \tag{6}$$

Here, $\Gamma_S(\phi) = 2\pi\nu_0|t^s_k|^2\cos(\phi/2)$ is the Josephson phase dependent strength of the intra-QD electron pairing induced by the coherent Andreev tunneling, ν_0 is the electron density of states in the leads, and $\mathcal{L}[\rho]$ is a Lindbladian operator in the high-voltage regime $eV \gg \varepsilon_0, \omega_0, k_BT$, which allows us to use the Born-Markov approximation [42,43]:

$$\mathcal{L}[\rho] = \frac{\Gamma}{2}\begin{cases}\{e^{-\frac{2\hat{x}}{\lambda}} d_\sigma d^\dagger_\sigma, \rho\} - 2e^{-\frac{\hat{x}}{\lambda}} d^\dagger_\sigma \rho d_\sigma e^{-\frac{\hat{x}}{\lambda}}, V > 0,\\ \{e^{-\frac{2\hat{x}}{\lambda}} d^\dagger_\sigma d_\sigma, \rho\} - 2e^{-\frac{\hat{x}}{\lambda}} d_\sigma \rho d^\dagger_\sigma e^{-\frac{\hat{x}}{\lambda}}, V < 0.\end{cases} \tag{7}$$

Here $\Gamma = 2\pi\nu_0|t^n_k|^2$ is the QD energy level width produced by a single electron tunneling between the STM tip and the

CNT. The quantum master equation (6) is justified in the deep subgap regime under the following assumptions: All relevant energies are smaller than the SC gap, $eV, k_BT, \varepsilon_0, \Gamma \ll \Delta$, and as a result all quasiparticle processes in the SC leads can be disregarded. This approximation results in the appearance of the second term in Eq. (6), responsible for the "proximity" effect.

Density matrix ρ acts in the finite Fock space of the twofold degenerate single-electron level in the QD. The four possible electronic states are $|0\rangle$, $|\sigma\rangle = d_\sigma^\dagger|0\rangle$ ($\sigma = \uparrow, \downarrow$), and $|2\rangle = d_\uparrow^\dagger d_\downarrow^\dagger|0\rangle$. In this representation the reduced density matrix ρ contains five nonzero elements: ρ_{00}, $\rho_{\uparrow\uparrow} = \rho_{\downarrow\downarrow} \equiv \rho_1$, ρ_{22}, ρ_{02}, and ρ_{20}. Using the normalization condition $\rho_{00} + 2\rho_1 + \rho_{22} = 1$ one can eliminate the ρ_1 component of the density matrix from further consideration. Therefore, the joint dynamics of the electronic and mechanical subsystems is determined by the matrix

$$\hat{\varrho} = \frac{1}{2}\begin{pmatrix} \rho_{22} - \rho_{00} & 2\rho_{20} \\ 2\rho_{02} & \rho_{00} - \rho_{22} \end{pmatrix}. \tag{8}$$

If the amplitude of the CNT displacement is larger than the amplitude of zero-point oscillation, one can treat the dynamics of the CNT bending as a classical with time evolution governed by Newton's equation. Introducing the dimensionless time units as $\omega_0 t \to t$ we obtain a closed system of the relevant equations for the CNT displacement x and matrix $\hat{\varrho}$ Eq. (8) in the following form:

$$\ddot{x} + Q^{-1}\dot{x} + x = \alpha + \alpha \mathrm{Tr}\{\sigma_3\hat{\varrho}\}, \tag{9}$$

$$\omega_0\dot{\hat{\varrho}} = -i[\varepsilon(x)\sigma_3 - \Gamma_S(\phi)\sigma_1, \hat{\varrho}] - \Gamma(x)\left(\hat{\varrho} - \frac{\kappa}{2}\sigma_3\right), \tag{10}$$

where dimensionless parameter $\alpha = F/\omega_0$, σ_i ($i = 1, 2, 3$) are the Pauli matrices, $\varepsilon(x) = \varepsilon_0 - \alpha x$, $\Gamma(x) = \Gamma \exp(-2x/\lambda)$, and $\kappa = \mathrm{sgn}(V)$. An environment induced damping of the mechanical subsystem is determined by the term $\propto Q^{-1}$, where $Q \sim 10^6$ [21] is the quality factor.

In the adiabatic limit, $\omega_0/\Gamma \ll 1$, we obtain $\hat{\varrho}(t)$ from Eq. (10), and the nonlinear part of Eq. (9) is presented in the following form (see details in Appendix):

$$\mathrm{Tr}\{\sigma_3\hat{\varrho}(t)\} \approx \kappa\left(1 - \frac{4\Gamma_S^2(\phi)}{D(x(t),\phi)}\right) + \dot{x}(t)\eta(x(t)), \tag{11}$$

where $D(x,\phi) = \Omega_R^2(x,\phi) + \Gamma^2(x)$, $\Omega_R(x,\phi) = 2\sqrt{\varepsilon^2(x) + \Gamma_S^2(\phi)}$ is the energy difference between two Andreev levels of the QD-SC subsystem. Notation Ω_R means that energy difference between two Andreev levels plays the similar role as the Rabi frequency in the two-level problem as will be discussed below. A mechanical friction coefficient $\eta(x)$, induced by interaction with the electronic degree of freedom, reads as

$$\eta(x) = \alpha\mathcal{I}(x)\left(\lambda^{-1}C_1(x) + \alpha\frac{\varepsilon(x)}{\Gamma^2(x)}C_2(x)\right). \tag{12}$$

Here, $\mathcal{I}(x) = \kappa 4\Gamma(x)\Gamma_S^2(\phi)/D(x,\phi)$ is the DC flow of electrons between the STM tip and SC leads, and

$$C_1(x) = \frac{6\Gamma^2(x) - 2\Omega_R^2(x)}{D^2(x,\phi)}, \tag{13}$$

$$C_2(x) = \frac{20\Gamma^2(x) + 4\Omega_R^2(x)}{D^2(x,\phi)}. \tag{14}$$

The frequency of a typical CNT-based resonator is $\omega_0 \sim 1$ GHz, while the amplitude of zero-point fluctuations is $x_0 \approx 2$ pm. Assuming $V_g \sim 100$ mV, $h \sim 10^{-7}$m, and the tunneling length $l \simeq 10^{-10}$ m we estimate dimensionless coupling constants to be $\alpha \sim 0.1$ and $\lambda^{-1} \sim 10^{-2}$.

After substituting Eq. (11) in Eq. (9), we found nonlinear equation for the CNT deformation local in time. In the limit $\alpha, \lambda^{-1} \ll 1$ a small shift of the equilibrium position (static solution) is obtained as

$$x_c = \alpha + \kappa\alpha\frac{4\varepsilon^2(0) + \Gamma^2}{D(0,\phi)} + O(\alpha^2, \alpha\lambda^{-1}). \tag{15}$$

The stability of the static solution is studied by linearizing Eq. (11). In the limit $\Gamma \gg \omega_0$, the time evolution of the small CNT deviation from its equilibrium position $\delta x(t) = x(t) - x_c$ is given by [44]

$$\delta\ddot{x} + (Q^{-1} - \eta(0))\delta\dot{x} + \delta x = 0. \tag{16}$$

The static solution x_c of the system at $\eta(0) > Q^{-1}$ becomes *unstable* with respect to the generation of mechanical oscillation with amplitude exponentially increasing in time. Development of instability results in the appearance of self-sustained mechanical oscillations, governed by the nonlinearity of r.h.s. Eq. (9).

Next, we analyze the influence of various parameters on the coefficient $\eta(0)$ which we call a pumping coefficient in what follows. First, we note that $\eta(0)$ linearly increases with the electromechanical coupling α and the DC flow $\propto\mathcal{I}(0)$. Moreover, the pumping coefficient $\eta(0)$ changes a sign depending on the direction of the electronic flow, i.e., the sign of eV. At $eV > 0$ ($\kappa = 1$) there is a flow of electrons from the STM tip to the SC leads, while at $eV < 0$ ($\kappa = -1$) there is a flow of holes in the same direction. At $|eV| \gg 2\varepsilon_0$, bias voltage affects the phenomenon under consideration solely by this means. Below we analyze the case of $eV > 0$ only.

The various dependencies of the pumping coefficient $\eta(0)$ on the parameters ϕ, $\Gamma/\Gamma_S(0)$, and $\varepsilon(0)$ obtained from Eqs. (12), (13), and (14) are shown in Fig. 2. Red color scheme in Fig. 2 indicates the regime of mechanical instability $\eta(0) > 0$, while blue scheme shows the region of the overdamped mechanical oscillations $\eta(0) < 0$. In the case $\varepsilon(0) = \varepsilon_0 = 0$, the pumping coefficient $\eta(0) \propto \kappa\alpha/\lambda$ is determined by the ratio between Γ and $\Gamma_S(\phi)$, since only the first term in Eq. (12) contributes. The pumping coefficient changes its sign when $\Gamma = \sqrt{4/3}\Gamma_S(\phi)$, see Fig. 2(a). If the dependence of the electron hopping on the amplitude of the CNT oscillations is negligible, i.e., $\lambda^{-1} = 0$, the pumping coefficient $\eta(0) \propto \kappa\alpha^2\varepsilon(0)$ is determined by the sign of $\varepsilon(0)$. Such behavior is illustrated in Fig. 2(b). General case, when both terms Eq. (13) and Eq. (14) contribute into the pumping coefficient Eq. (12), is shown in Figs. 2(c) and 2(d). Figures 2(c) and 2(d) illustrate the cases of "posi-

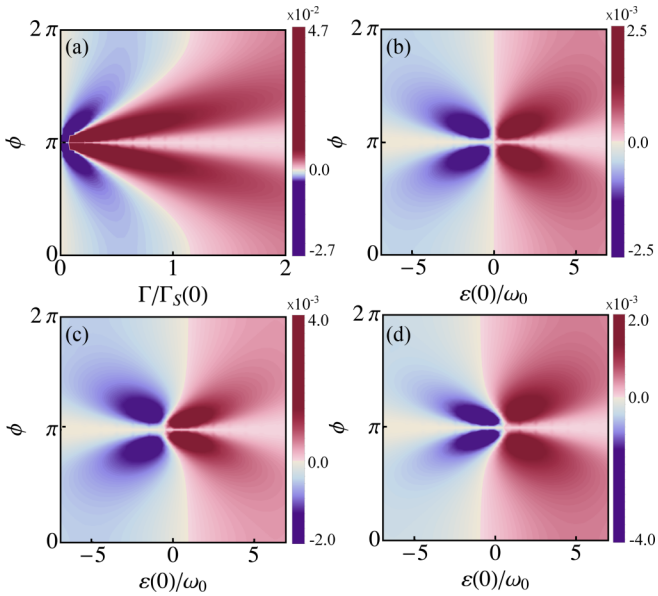

FIG. 2. Phase diagrams of the mechanical instability showing pumping coefficient $\eta(0)$ as a function of the Josephson phase difference ϕ, the QD level width $\Gamma/\Gamma_S(0)$, and the QD energy level $\varepsilon(0)/\omega_0$ for: (a) $\alpha = 0.2$, $\lambda^{-1} = 0.05$, and $\varepsilon(0) = 0$ [when only Eq. (13) contributes into $\eta(0)$]; (b) $\alpha = 0.2$, $\Gamma/\Gamma_S(0) = 0.3$, and $\lambda^{-1} = 0$ [when only Eq. (14) contributes into the pumping coefficient]; and for general case $\Gamma/\Gamma_S(0) = 0.3$, $\lambda^{-1} = 0.05$ when (c) $\alpha = 0.2$ and (d) $\alpha = -0.2$. The red and blue color schemes indicate the mechanical instability ($\eta > 0$) and the damping ($\eta < 0$) regimes, respectively. All diagrams are calculated for the case $Q^{-1} = 0$ and $\kappa = 1$.

tive" ($\alpha > 0$) and "negative" ($\alpha < 0$) electrostatic interaction, respectively.

The origin of the pumping processes and corresponding mechanical instability can be qualitatively explained as follows: Since two electronic states $|0\rangle$ and $|2\rangle$ in the QD are not the eigenstates of the QD-SC subsystem, the quantum Rabi oscillations emerge with a frequency proportional to the energy difference between Andreev levels $\Omega_R(x, \phi)$. These Rabi oscillations occur in the form of periodic in time single-Cooper pair transfer between SC leads and the QD. However, an incoherent single electron tunneling from the STM tip to the QD can interrupt the coherent oscillations as well as resume them.

As this takes place, the averaged charge in the QD is governed by the interplay between two processes: (i) coherent Rabi oscillations and (ii) an incoherent single electron tunneling. Both processes and their main characteristics, $\Gamma(x)$ and $\Omega_R(x)$, are controlled by the CNT displacement and vary in time if $\delta\dot{x}(t) \neq 0$. Such variations give rise to a correction of the average charge in the QD that is proportional to the velocity of the QD, thereby generating effective friction force. We note that the amplitude of the effective friction force is determined by two terms [see Eq. (12)], where the first term is induced by the time variation of the hopping amplitude of single electron tunneling $\dot{\Gamma}(x(t)) \propto \lambda^{-1}\dot{x}$, while the second term is generated by the time variation of the Rabi frequency $\dot{\Omega}_R(x(t)) \propto \alpha\varepsilon(0)\dot{x}$.

IV. DC ELECTRIC CURRENT

The self-sustained oscillations affect the DC current flow between the STM tip and SC leads. This phenomenon allows one to verify the mechanical instability through the electric current measurement.

In the high-voltage regime $eV > 2|\varepsilon_0|$, electron transfer from the CNT-QD to the STM tip is blocked. The instantaneous current between normal metal and the CNT-QD is equal to twice the product (account spin degree of freedom) of the transition rate ($\Gamma \exp[-2x/\lambda]$) that determines the number of electron transfer per second and sum of probabilities of the QD being in the empty (ρ_{00}) or single occupied (ρ_1) states, see, e.g., Refs. [45,46]. The DC current in the adiabatic regime reads as follows:

$$I_N(x(t)) = 2e\Gamma e^{-\frac{2x(t)}{\lambda}}\kappa[\rho_{00}(t) + \rho_1(t)] \equiv e\Gamma(x(t))(\kappa - \mathrm{Tr}\{\sigma_3\hat{\varrho}(t)\}). \quad (17)$$

If the pumping coefficient $\eta(0) < Q^{-1}$, the mechanical oscillations of the CNT are damped, and the DC electric current is expressed as (see Appendix for details)

$$I_N(0) = 4\kappa e\Gamma\frac{\Gamma_S^2(\phi)}{\varepsilon^2(0) + \Gamma_S^2(\phi) + \Gamma^2/4}. \quad (18)$$

This expression coincides with the DC current obtained in the absence of electromechanical interaction. Such dependence is shown in Fig. 3(a). The DC current strongly depends on the Josephson phase difference ϕ and the QD energy level $\varepsilon(0)$. The current reaches its maximum at $\varepsilon(0) = 0$ and vanishes at $\phi = \pi$. Besides, $I_N(0)$ is proportional to $\propto\Gamma\Gamma_S^2$, revealing Andreev tunneling [47] since only two electrons (the Cooper pair) can tunnel from the QD to the SC leads.

In the regime of mechanical instability $\eta(0) > Q^{-1}$, the static solution becomes unstable and CNT vibrations develop into pronounced self-sustained oscillations of finite amplitude. As a result, the current exhibits periodic oscillations with the frequency ω_0. The averaged over the period of mechanical oscillations DC current is obtained numerically and the result is presented in Fig. 3(b). The projections of I_N at fixed ϕ and $\varepsilon(0)$ are presented in Figs. 3(c) and 3(d), respectively. As one can see in Fig. 3, pronounced self-sustained oscillations of the CNT-QD suppress the charge current in the region of parameters obeyed $\eta(0) > Q^{-1}$ condition. The strength of this current suppression depends on the amplitude of the CNT self-oscillations and correspondingly on the pumping strength $\eta(0)$.

Qualitatively, the mechanically induced DC current suppression can be understood in the adiabatic limit $\omega_0 \ll \Gamma$, when the regime of the self-sustained oscillations is achieved. Thus, the DC current can be approximated as $I_N(x(t)) \approx I_N(0) + (x^2(t)/2)(d^2I_N/dx^2)$. In the above expression $x(t)$ can be presented as $x = A\cos(\omega_0 t + \chi)$. Then, correction to the static DC current generated by self-sustained oscillations reads as $(A^2/4)d^2I_N/dx^2$ after averaging over the period of mechanical oscillations. Coefficient d^2I_N/dx^2 depends on various parameters of the system. Under the considered set of parameters, for which numerical results are presented in Fig. 3, d^2I_N/dx^2 gives a negative correction and results in the suppression of the DC current.

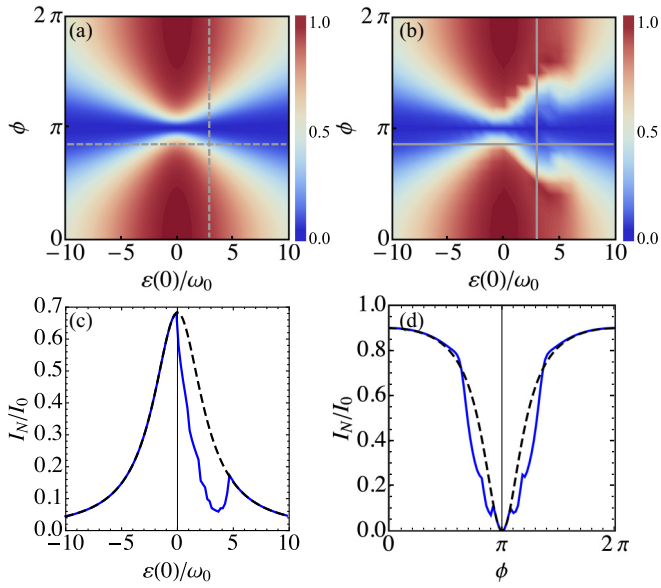

FIG. 3. DC electric current I_N/I_0 normalized to the maximum of static current $I_0 = e\Gamma$ as a function of the Josephson phase difference ϕ and the QD energy level $\varepsilon(0)/\omega_0$ at $\Gamma/\Gamma_S(0) = 0.3$ for the cases: (a) $\alpha = 0$ and (b) $\alpha = 0.2$. Dashed and solid gray lines indicate projections of the DC current at fixed $\phi = 2.7$ and fixed $\varepsilon(0)/\omega_0 = 3$, respectively. These projections are presented in panels (c) and (d), where the charge current $[I_N(0) = e\mathcal{I}(0)]$ at $\alpha = 0$ is shown by black dashed lines, and the DC current at $\alpha = 0.2$ is shown by the blue (solid) lines. Current in the pumping regime is calculated numerically from Eqs. (18), (9), and (10) by averaging over the period of mechanical vibrations. All figures are obtained for $Q = 10^6$, $\kappa = 1$, and $\lambda^{-1} = 0.05$.

V. SUMMARY AND DISCUSSIONS

We predict the phenomenon of mechanical instability and corresponding self-sustained oscillations in a hybrid nano-electromechanical device consisting of a carbon nanotube suspended between two SC leads and placed near a voltage-biased normal STM tip. Such an effect is based on a peculiar interplay of the coherent quantum-mechanical Rabi oscillations induced by the Andreev tunneling between the CNT and SC leads, and an incoherent single electron tunneling between the STM tip and CNT. We obtain that the observed mechanical instability and self-sustained oscillations of finite amplitude are determined by two parameters: the relative position of the single-electron energy level and the Josephson phase difference between the SC leads. Numerical analysis demonstrates that the predicted mechanical instability develops into pronounced self-sustained bending oscillations of the CNT resonator which, in its turn, result in a suppression of the DC electric current flowing between the STM tip and SC leads. This effect allows one to detect the predicted mechanical instability through the DC current measurement. A SQUID sensitivity to an external magnetic field can be achieved by using proposed nanomechanical Andreev device through the control of the Josephson phase difference by a magnetic flux.

ACKNOWLEDGMENTS

This work was supported by the Institute for Basic Science in Korea (IBS-R024-D1). This work was supported by Project Code No. (IBS-R024-D1) and the Korea Institute for Advanced Study (KIAS) funded by the Korean government (MSIT). L.Y.G. and R.I.S. thank the IBS Center for Theoretical Physics of Complex Systems for their hospitality. M.V.F. acknowledges the partial financial support of the Ministry of Science and Higher Education of the Russian Federation in the framework of the State Program (Project No. 0718-2020-0025).

APPENDIX: REDUCED DENSITY MATRIX APPROACH

Here we would like to present the details of the derivation of Eq. (11). Using notations $R_i = \mathrm{Tr}\{\sigma_i\hat{\varrho}\}$ and $\vec{R} = (R_1, R_2, R_3)^T$, master equation (10) can be rewritten in the following form (in terms of dimensionless time $\omega_0 t$ and displacement x)

$$\omega_0\dot{\vec{R}} = \hat{A}\vec{R} + \kappa\Gamma(x)\vec{e}_3, \tag{A1}$$

where operator $\hat{A}$ reads

$$\hat{A} = \begin{pmatrix} -\Gamma(x) & -2\varepsilon(x) & 0 \\ 2\varepsilon(x) & -\Gamma(x) & 2\Gamma_S(\phi) \\ 0 & -2\Gamma_S(\phi) & -\Gamma(x) \end{pmatrix}, \tag{A2}$$

and $\vec{e}_3 = (0, 0, 1)^T$.

In the adiabatic limit $\omega_0 \ll \Gamma$, we assume that solution of the reduced density matrix can be presented as a series $\vec{R}(t) \approx \vec{R}^{(0)}(x(t)) + \dot{x}(t)(\omega_0/\Gamma)\vec{R}^{(1)}(t) + \ldots$. Substituting this ansatz into Eq. (A1) we get

$$\hat{A}\vec{R}^{(0)} = -\kappa\Gamma(x)\vec{e}_3, \tag{A3}$$

from which one can obtain the stationary solution of Eq. (10):

$$R_1^{(0)} = -\kappa\frac{4\Gamma_S(\phi)\varepsilon(x)}{D}, \quad R_2^{(0)} = \kappa\frac{2\Gamma_S(\phi)\Gamma(x)}{D}, \tag{A4}$$

$$R_3^{(0)} = \kappa\frac{4\varepsilon^2(x) + \Gamma^2(x)}{D}. \tag{A5}$$

After substitution of the Eqs. (A4) and (A5) in Eq. (A1), we obtain the first order correction to the reduced density matrix over small parameter $\omega_0/\Gamma \ll 1$:

$$\frac{d}{dx}\vec{R}^{(0)}(x) = \frac{1}{\Gamma}\hat{A}\vec{R}^{(1)}. \tag{A6}$$

A mechanical friction coefficient induced by the interaction with the electronic degree of freedom, second term in Eq. (11), is obtained by solving algebraic equation (A6).

[1] S. Schmid, L. G. Villanueva, and M. L. Roukes, *Fundamentals of Nanomechanical Resonators* (Springer, Cham, 2016).

[2] R. G. Knobel and A. N. Cleland, Nature (London) **424**, 291 (2003).

[3] M. P. Blencowe, Science **304**, 56 (2004).
[4] V. Sazonova, Y. Yaish, H. Üstünel, D. Roundy, T. A. Arias, and P. L. McEuen, Nature (London) **431**, 284 (2004).
[5] B. Lassagne, D. Garcia-Sanches, A. Aguasca, and A. Bachtold, Nano Lett. **8**, 3735 (2008).
[6] A. Hüttel, G. Steele, B. Witkamp, M. Poot, L. Kouwenhoven, and H. S. J. van der Zant, Nano Lett. **9**, 2547 (2009).
[7] X. M. H. Huang, C. A. Zorman, M. Mehregany, and M. L. Roukes, Nature (London) **421**, 496 (2003).
[8] M. P. Blencowe, Phys. Rep. **395**, 159 (2004).
[9] K. L. Ekinci and M. L. Roukes, Rev. Sci. Instrum. **76**, 061101 (2005).
[10] A. N. Cleland, *Foundations of Nanomechanics* (Springer, New York, 2002).
[11] P. Arrangoiz-Arriola, E. A. Wollack, Zh. Wang, M. Pechal, W. Jiang, T. P. McKenna, J. D. Witmer, R. Van Laer, and A. H. Safavi-Naeini, Nature (London) **571**, 537 (2019).
[12] J. Hauss, A. Fedorov, C. Hutter, Al. Shnirman, and G. Schön, Phys. Rev. Lett. **100**, 037003 (2008).
[13] M. D. LaHayae, J. Suh, P. M. Echternach, K. C. Schwab, and M. L. Roukes, Nature (London) **459**, 960 (2009).
[14] C. Urgell, W. Yang, S. L. De Bonis, C. Samanta, M. J. Esplandiu, Q. Dong, Y. Jin, and A. Batchtold, Nat. Phys. **16**, 32 (2020).
[15] G. Sonne, M. E. Pena-Aza, L. Y. Gorelik, R. I. Shekhter, and M. Jonson, Phys. Rev. Lett. **104**, 226802 (2010).
[16] P. Stadler, W. Belzig, and G. Rastelli, Phys. Rev. Lett. **117**, 197202 (2016).
[17] G. Rastelli and M. Governale, Phys. Rev. B **100**, 085435 (2019).
[18] L. Y. Gorelik, A. Isacsson, Y. M. Galperin, R. I. Shekhter, and M. Jonson, Nature (London) **411**, 454 (2001); A. Isacsson, L. Y. Gorelik, R. I. Shekhter, Y. M. Galperin, and M. Jonson, Phys. Rev. Lett. **89**, 277002 (2002).
[19] L. Y. Gorelik, A. Isacsson, M. V. Voinova, B. Kasemo, R. I. Shekhter, and M. Jonson, Phys. Rev. Lett. **80**, 4526 (1998).
[20] Ya. M. Blanter, O. Usmani, and Yu. V. Nazarov, Phys. Rev. Lett. **93**, 136802 (2004).
[21] G. A. Steele, A. Hüttel, B. Witkamp, M. Poot, H. B. Meerwaldt, L. P. Kouwenhowen, and H. S. J. van der Zant, Science **325**, 1103 (2009).
[22] D. R. Schmid, P. L. Stiller, C. Strunk, and A. Hüttel, Applied Phys. Lett. **107**, 123110 (2015).
[23] D. R. Schmid, P. L. Stiller, C. Strunk, and A. Hüttel, New J. Phys. **14**, 083024 (2012).
[24] K. Willick and J. Baugh, Phys. Rev. Research **2**, 033040 (2020).
[25] S. Etaki, M. Poot, I. Manhboob, K. Onomitsu, H. Yamaguchi, and H. S. J. van der Zant, Nat. Phys. **4**, 785 (2008).
[26] B. H. Schneider, S. Etaki, H. S. J. van der Zant, and G. A. Steele, Sci. Rep. **2**, 599 (2012).
[27] A. V. Parafilo, I. V. Krive, R. I. Shekhter, and M. Jonson, Low Temp. Phys. **38**, 273 (2012) [Fiz. Nizk. Temp. **38**, 348 (2012)].
[28] T. Novotny, A. Rossini, and K. Flensberg, Phys. Rev. B **72**, 224502 (2005).
[29] A. Zazunov, D. Feinberg, and T. Martin, Phys. Rev. Lett. **97**, 196801 (2006).
[30] J. Sköldberg, T. Löfwander, V. S. Shumeiko, and M. Fogelström, Phys. Rev. Lett. **101**, 087002 (2008).
[31] C. Padurariu, C. J. H. Keijzers, and Yu. V. Nazarov, Phys. Rev. B **86**, 155448 (2012).
[32] A. Zazunov and R. Egger, Phys. Rev. B **81**, 104508 (2010).
[33] A. V. Parafilo, I. V. Krive, R. I. Shekhter, Y. W. Park, and M. Jonson, Low Temp. Phys. **39**, 685 (2013).
[34] A. V. Parafilo, I. V. Krive, R. I. Shekhter, Y. W. Park, and M. Jonson, Phys. Rev. B **89**, 115138 (2014).
[35] J. Baranski and T. Domanski, J. Phys.: Condens. Matter **27**, 305302 (2015).
[36] A. F. Andreev, Zh. Eksp. Teor. Fiz. **46**, 1823 (1964) [Sov. Phys. JETP. **19**, 1228 (1964)].
[37] I. O. Kulik, Zh. Eksp. Teor. Fiz. **57**, 1745 (1969) [Sov. Phys. JETP **30**, 944 (1970)].
[38] V. S. Shumeiko, G. Wendin, and E. N. Bratus', Phys. Rev. B **48**, 13129 (1993).
[39] L. Y. Gorelik, V. S. Shumeiko, R. I. Shekhter, G. Wendin, and M. Jonson, Phys. Rev. Lett. **75**, 1162 (1995).
[40] F. S. Bergeret, P. Virtanen, T. T. Heikkilä, and J. C. Cuevas, Phys. Rev. Lett. **105**, 117001 (2010).
[41] Y. V. Nazarov and Ya. M. Blanter, *Quantum transport: Introduction to Nanoscience* (Cambridge University Press, New York, 2009).
[42] T. Novotny, A. Donarini, and A.-P. Jauho, Phys. Rev. Lett. **90**, 256801 (2003).
[43] D. Fedorets, L. Y. Gorelik, R. I. Shekhter, and M. Jonson, Phys. Rev. Lett. **95**, 057203 (2005); New J. Phys. **7**, 242 (2005).
[44] In Eq. (16) we ignore small renormalization of the frequency of mechanical oscillations.
[45] B. Hiltscher, M. Governale, and J. König, Phys Rev. B **86**, 235427 (2012).
[46] S. Pfaller, A. Donarini, and M. Grifoni, Phys. Rev. B **87**, 155439 (2013).
[47] J. Gramich, A. Baumgartner, and C. Schönenberger, Phys. Rev. Lett. **115**, 216801 (2015).